Effects of host heterogeneity on epidemiological dynamics are mediated by how host infectiousness is determined

Jacob A. Cohen[1], Andrew D. Dean[1], Mark E. Viney[1], Andy Fenton[1]

[1]Department of Evolution, Ecology and Behaviour, Institute of Infection, Veterinary and Ecological Sciences, University of Liverpool, Liverpool L69 7ZB, UK

Abstract

It is well established that heterogeneities in host susceptibility and infectiousness can affect population-level parasite transmission. However, the role played by the underlying 'infectiousness determination scenario', or how infectious a newly infected host (the 'recipient') becomes upon infection, in mediating the effects of host heterogeneity on parasite transmission is unknown.

Broadly, host infectiousness may be an inherent, pre-determined trait of the recipient (which we call 'Recipient-Dependent' (RD)), or it may be determined by the infectiousness of the 'donor' host that infected them (which we call 'Donor-Dependent' (DD)). To investigate how these alternative infectiousness determination scenarios mediate the epidemiological consequences of host heterogeneity we developed two Susceptible-Infected compartmental models which incorporate host heterogeneity in both susceptibility and infectiousness, under the contrasting RD and DD scenarios. We then quantified how changing initial population-level heterogeneity affected three epidemiological measures in each case: the basic reproduction number (R_0), temporal changes in heterogeneity, and equilibrium host abundance. We found that the primary driver of R_0 differs between the two scenarios – covariance between host susceptibility and infectiousness drives R_0 in the RD scenario, versus maximum infectiousness in the DD scenario. Heterogeneity stayed the same over time in both scenarios, though there were differences between the scenarios in the consequences of host heterogeneity on equilibrium host abundance. Overall, the findings we present demonstrate that the infectiousness determination scenario can change epidemiological outcomes considerably and should be accounted for when modelling host heterogeneities in parasite transmission.

Key words

disease ecology; host heterogeneity; parasite transmission; susceptibility; infectiousness; R_0

Introduction

It is well recognised that individuals can vary substantially in their propensity to be infected by, and to transmit, parasites [1]. This individual-level host heterogeneity can have significant effects on the transmission of parasites and thus impact the dynamics of infection in host populations [2, 3]. One such example of individual-level host heterogeneity which is known to affect parasite transmission is superspreaders – hosts that are disproportionally responsible for transmission of an infection in a population [4]. These transmission heterogeneities can arise through variation in one or more epidemiologically-relevant traits. Specifically, parasite transmission is a function of host susceptibility (the host's propensity to become infected following parasite exposure), host infectiousness (the capacity of an infected host to transmit parasites) and contact rate (the rate of transmission-relevant contacts, dependent on the transmission mode of the parasite in question) [5].

Variation in these epidemiologically-relevant traits can alter parasite transmission dynamics across the host population [6-10]. For example, modelling has shown that heterogeneity in susceptibility can reduce parasite transmission in a population [11], heterogeneity in host infectiousness can increase variability in the probability an epidemic will occur [12] and heterogeneity in contact rate can slow transmission speeds and reduce overall epidemic severity [13]. Importantly, these host heterogeneities can exist simultaneously, and potentially covary, raising the question of how these so-called 'coupled heterogeneities' [14] affect parasite transmission. Previous modelling has shown that not only can multiple heterogeneities affect transmission dynamics, but that interactions between these heterogeneities can as well [15-17]. Indeed, covariation between host heterogeneities can both positively and negatively impact the parasite's basic reproduction number, R_0, depending on the traits involved and directionality of the covariation [14, 18].

Generally ignored, yet fundamental to understanding the effect of coupled heterogeneities on parasite transmission, is how individual-level, epidemiologically-relevant traits are determined. In particular, there has been little consideration of how a host's infectiousness is determined as it becomes infectious, or the 'infectiousness determination scenario'. Broadly, there are two possible scenarios. In the first, which we call **recipient-dependent (RD)**, a susceptible 'recipient' host's subsequent infectiousness is assumed to be a fixed, pre-determined characteristic of that individual, as might occur when a host's genotype determines their infectiousness. In the second, which we call **donor-dependent (DD)**, a recipient host's subsequent infectiousness is assumed to be determined by the 'donor' host that infected them, for example if the parasite load the recipient receives determines their infectiousness (*i.e.*, highly infectious hosts tend to generate other highly infectious hosts upon infection) [19, 20]. Despite these divergent scenarios likely leading to differing patterns in host

infectiousness in the population, and thus different transmission outcomes, most modelling studies of the impacts of host heterogeneity tend not to explicitly consider which underlying infectiousness scenario they have employed. The majority implicitly assume RD infectiousness determination, for example by pre-assigning susceptibility and infectiousness values to individuals (e.g., [11, 16-18]), although occasionally DD-like models have been used [19].

How the infectious determination scenario mediates the effects of host heterogeneities on population-level parasite transmission has not been tested. Here we explore this issue by focusing on host heterogeneities in susceptibility and infectiousness, two traits which are likely to be determined by similar physiological and immunological mechanisms, and thus likely to be linked [21]. We develop two Susceptible-Infected (SI) compartmental models that incorporate host heterogeneity in susceptibility and infectiousness, one assuming the RD scenario and the other assuming the DD scenario. We analyse these models to determine how the underlying infectiousness scenario affects the relationship between host heterogeneities in susceptibility and infectiousness and population-level parasite transmission as well as its effect on host population dynamics.

Methods

Model Framework

The standard density-dependent SI model in a homogeneous population of size N divided into susceptible (S) and infected (I) subpopulations [22] is given by

$$\frac{dS}{dt} = bN - \beta SI - dS, \tag{1}$$

$$\frac{dI}{dt} = \beta SI - (d + \alpha)I, \tag{2}$$

where $N = S + I$, b is the birth rate, d is the baseline mortality rate and α is the parasite-induced mortality rate. Although often written as a simple constant, the transmission coefficient β in fact incorporates both contact rate (κ) and infection probability given a contact (ν) [23], yielding

$$\beta = \kappa\nu. \tag{3}$$

The infection probability ν can be further partitioned into the product of recipient susceptibility (σ) and donor infectiousness (ι),

$$\nu = \sigma\iota, \tag{4}$$

where σ and ι take values in [0,1], with higher values representing greater susceptibility or greater infectiousness respectively. Thus, host heterogeneity in susceptibility and infectiousness can be incorporated by dividing the population into subpopulations comprising those individuals that share the same values of susceptibility and infectiousness. Precisely how this is done depends on whether there is a RD or DD infectiousness determination.

Recipient-dependent (RD)

Here susceptible recipient hosts are assigned to an infected group based on a fixed, pre-determined trait inherent to that individual. Supposing that there are n unique pairs of trait values (σ_j, ι_j), $1 \leq j \leq n$, we divide the population into n susceptible subpopulations S_j and n infected subpopulations I_j, where the jth subpopulations share the jth trait pair. Thus, a RD heterogeneous analogue of Equations (1)-(2) is

$$\frac{dS_j}{dt} = \frac{bN}{n} - \kappa\sigma_j S_j \sum_{m=1}^{n} \iota_m I_m - dS_j, \tag{5}$$

$$\frac{dI_j}{dt} = \kappa\sigma_j S_j \sum_{m=1}^{n} \iota_m I_m - (d+\alpha)I_j, \tag{6}$$

where we have additionally assumed that birth rate b, baseline mortality rate d, and parasite-induced mortality rate α are equal across subpopulations. For the sake of simplicity, births are evenly distributed across susceptible subpopulations, effectively assuming non-inherited host heterogeneity, a phenomenon that has been previously observed, for example in *Daphnia magna* [24]. We emphasise that in this scenario, the fixed traits of individuals determine the susceptible and infected subpopulation to which they belong, so all individuals from a susceptible subpopulation move to the same infected subpopulation upon infection.

Donor-dependent (DD)

In this alternative scenario, susceptible recipient hosts do not have an infectiousness trait until they become infected. Hence, we divide the susceptible subpopulation into n_S subpopulations S_j, each with susceptibility σ_j, $1 \leq j \leq n_S$. Upon infection, individuals are assigned the infectiousness of the donor host that infected them. We therefore define $I_{j,k}$ to be those individuals with susceptibility σ_j that were infected by an individual with infectiousness ι_k, $0 \leq k \leq n_I$, and so now share that same infectiousness value. Thus a DD heterogeneous analogue of Equations (1)-(2) is

$$\frac{dS_j}{dt} = \frac{bN}{n_S} - \kappa\sigma_j S_j \sum_{m=1}^{n_I} \sum_{l=1}^{n_S} \iota_m I_{l,m} - dS_j, \tag{7}$$

$$\frac{dI_{j,k}}{dt} = \kappa\sigma_j \iota_k S_j \sum_{l=1}^{n_S} I_{l,k} - (d+\alpha)I_{j,k}. \tag{8}$$

b, d and α are again assumed to be equal for all infected groups. Unlike the RD model, the infected subpopulation that the recipient host will join is not pre-determined before infection, so individuals in the same susceptible subpopulation do not always move to the same infected subpopulation upon infection. Hence, though the RD model has equal numbers of both susceptible and infected subpopulations, the DD model has n_s susceptible groups and $n_S n_I$ infectious groups.

Equations (7)-(8), which will be useful when considering the heterogeneity of the population, can be simplified by defining $I_k = \sum_{j=1}^{n_S} I_{j,k}$, i.e., the sum of all individuals with the same infectiousness trait, regardless of their initial susceptibility trait. Summing Equation (8) over $0 \leq j \leq n_S$ yields

$$\frac{dS_j}{dt} = \frac{bN}{n_S} - \kappa\sigma_j S_j \sum_{m=1}^{n_I} \iota_m I_m - dS_j, \tag{9}$$

$$\frac{dI_k}{dt} = \kappa\iota_k I_k \sum_{m=1}^{n_S} \sigma_m S_m - (d+\alpha) I_k, \tag{10}$$

describing the dynamics of all infected individuals with infectiousness ι_k. This form of the system is useful if the prior susceptibility of infected individuals is unimportant, for example when calculating R_0. Note that we have used the same notation in the RD and the DD models to define similar but not precisely equivalent variables, and therefore will rely on context to ensure it is clear which is being referred to throughout the remainder of this work.

Quantifying population-level heterogeneity

Population-level heterogeneity (hereafter referred to simply as 'heterogeneity') was quantified by following a method used in [25], applicable to a wide range of systems and capable of dealing with multiple traits and missing values [26]. Heterogeneity calculations were undertaken in the context of two-dimensional σ, ι trait space, in which susceptibility (σ) and infectiousness (ι) form the two axes.

We first calculated the abundance-weighted centroid (c, hereafter referred to as the 'centroid') of the population, given simply as the population mean of each trait ($\bar{\sigma}$ and $\bar{\iota}$, Figure 1A & C). We then calculated the heterogeneity score, h, by finding the mean abundance-weighted, Euclidean distance to the centroid (e.g. z_1 in Figure 1B, z_{11} in Figure 1D) of all subpopulations. We calculated initial heterogeneity using the initial abundances of the subpopulations and final (equilibrium) heterogeneity using equilibrium subpopulation abundances.

We note that the calculation of heterogeneity differs somewhat between the RD and DD models, specifically in how subpopulations were grouped, and abundances calculated. For the RD model, where all individuals in the same susceptible subpopulation move to the same infected subpopulation, we summed the abundances of the corresponding susceptible and infected subpopulations. These grouped subpopulations were then used to calculate h.

For the DD model, however, the subsequent infectiousness of a susceptible was not pre-determined, so susceptible and infected subpopulations could not be summed to generate a combined abundance. Instead, each infected subpopulation's Euclidean distance to the centroid was calculated using both its σ and ι values (e.g. I_{11} in Figure 1D) while, because susceptible subpopulations only had a σ value,

their distance to the centroid was calculated in a single dimension (e.g. S_1 in Figure 1D). Thus there were no grouped subpopulations used in calculating h.

The formulae for heterogeneity calculations for both the RD and DD models can be found in the Supplementary Information (SI).

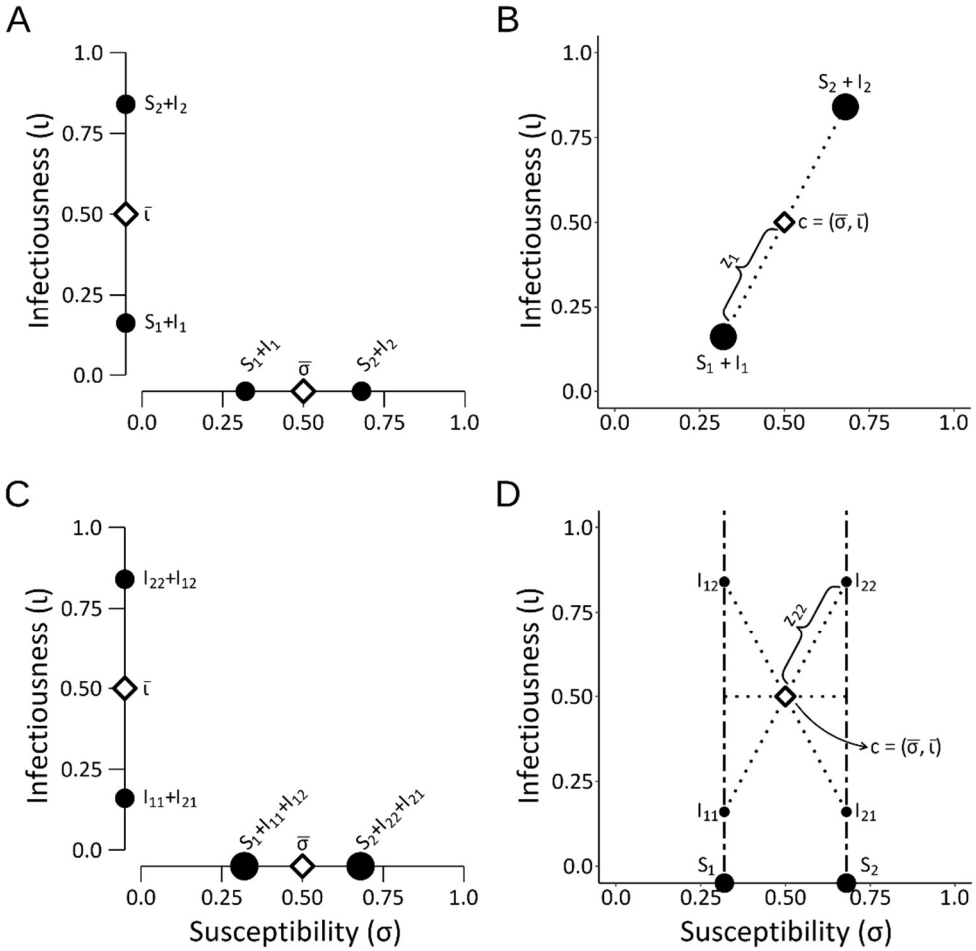

Figure 1. Schematic representation of the calculation of population-level heterogeneity score. A) RD model. The centroid (c) is found by calculating the population mean for susceptibility and infectiousness values in a single dimension. B) Heterogeneity for the RD model is then calculated by finding the mean Euclidean distance (z_i), weighted by the abundance of each group (represented by the diameter of the circle), to the centroid (c) found in panel A. C) DD model. The centroid (c) is found by calculating the population mean for susceptibility and infectiousness values in a single dimension. D) Heterogeneity for the DD model is then calculated by finding the mean of the Euclidean distances (z_i) of the infected groups to the centroid and the distance in a single dimension (σ dimension) of the susceptible groups, weighted by the abundance of each group. The values for $S_1$and S_2 form lines rather than points in σ, ι trait space as they have no infectiousness values.

Model Analyses

We analysed both the RD and DD models under three scenarios:

1) *Bipartite heterogeneity*
   The population is split into subpopulations corresponding to two distinct pairs of values of susceptibility and infectiousness.
2) *Tripartite isometric heterogeneity*
   The population is split into subpopulations corresponding to three distinct pairs of susceptibility and infectiousness values, equidistant from each other in σ, ι trait space.
3) *Tripartite non-isometric heterogeneity*
   The population is split into subpopulations corresponding to three distinct pairs of susceptibility and infectiousness values, not necessarily equidistant in σ, ι trait space.

In what follows we focus on the first of these, with the analyses for both tripartite heterogeneity scenarios presented in the SI.

For all quantitative analyses we set initial abundances of all susceptible subpopulations to 49 and all infected subpopulations to $\frac{1}{n}$ (RD) or $\frac{1}{n_S}$ (DD). We also set initial mean population trait values for both susceptibility and infectiousness to 0.5. Thus $\sigma_2 = 1 - \sigma_1$ and $\iota_2 = 1 - \iota_1$. All other parameter values were the same for all analyses (Table 1). By varying σ_1 and ι_1, we therefore varied the initial population heterogeneity while maintaining the same initial mean population trait values. Hence, the effects of changes in heterogeneity were decoupled from the effects of changes in initial mean population trait values.

Table 1. Parameter values for all analyses of RD and DD models.

Model parameter	Definition	Value
κ	Contact rate per individual per time	0.5
b	Birth rate per time	1.5
d	Mortality rate per time	1
α	Parasite-induced mortality rate per time	0.7

For each scenario we generated a range of unique combinations of σ and ι trait values (n = 2,601 bipartite heterogeneity). We then used these unique combinations of trait values to analyse both the RD and DD models to understand how heterogeneity in susceptibility and infectiousness affected

three key descriptors of epidemiological dynamics: (I) the basic reproduction number (R_0; a measure of epidemic potential) [22], (II) change in heterogeneity between the initial and final state of the system (indicating how heterogeneity changes with epidemic progression), and (III) equilibrium host population abundances (quantifying the impact of the parasite on the host population).

Calculating R_0

R_0 is a measure of the epidemic potential of a system. It predicts the risk of an epidemic occurring, as well as the size and severity of that epidemic [22, 27], and also the effort needed to control and eliminate a parasite from a population [28]. Thus, understanding the effect of heterogeneity on R_0 provides considerable insight into how host heterogeneity in susceptibility and infectiousness affects parasite transmission through a population.

We calculated R_0 for the RD and DD models using next generation matrices [29] (calculations in SI).

RD:

$$R_0 = \frac{\kappa}{d+\alpha}\sum_{j=1}^{n}\sigma_j \iota_j S_j \,. \tag{11}$$

DD:

$$R_0 = \frac{\kappa\bar{\sigma}\iota_{\max}N}{d+\alpha}, \tag{12}$$

where $\iota_{\max}$ is the maximum infectiousness value across all subpopulations.

Equilibrium Analyses

When possible we calculated the equilibrium solutions of Equations (5)-(8) analytically. For parameter values for which this was not possible, we instead solved the system numerically over a period of 50,000 time steps, which was sufficiently long to reach equilibrium. Any subpopulation with susceptibility $\sigma = 0$ (i.e., completely resistant to infection) experiences unbounded growth, and so such cases were omitted from equilibrium analyses.

We also used these equilibrium solutions to calculate equilibrium population-level heterogeneity to test whether the population-level heterogeneity changed with epidemiological progress.

Software packages

All plots were generated in R [30] using packages ggplot2 [31], ggforce [32], scales [33], showtext [34], pBrackets [35], patchwork [36] and latex2exp [37]. All equilibrium analyses were conducted using Mathematica [38]. Heterogeneity and R_0 values were calculated in R [30].

Results

The results for the analyses of the bipartite heterogeneity scenarios are presented here. The results for the analyses of the tripartite heterogeneity scenarios were broadly consistent with those of their bipartite heterogeneity counterparts and are described in the SI.

Heterogeneity and R_0

Recipient-dependent

For the RD model, increasing initial heterogeneity has contrasting effects on R_0 relative to the homogenous case ($h = 0$). Depending on the population-level covariance between susceptibility and infectiousness values, R_0 may increase (Figure 2A, red points), decrease (Figure 2A, blue points) or remain the same (Figure 2A, yellow points) as heterogeneity increases. Mapping R_0 values onto σ, ι trait space (Figure 2C), where the two subpopulations are mirrored across the centre point ($\sigma_2 = 1 - \sigma_1$ and $\iota_2 = 1 - \iota_1$), shows that R_0 remains unchanged from the homogeneous state, even at high levels of heterogeneity, if that heterogeneity is in one trait only (Figure 2C yellow shading).

R_0 increases relative to the homogenous state when there is positive covariation between susceptibility and infectiousness (Figure 2C, Supplementary Equation (S13)). The largest R_0 value occurs when one group has maximal infectiousness and susceptibility values of 1, while the other group has values of 0 for both; i.e., the groups lie at extremes of the positive diagonal in σ, ι trait space (Figure 2C). Conversely, R_0 is reduced relative to the homogenous case when there is negative covariation between susceptibility and infectiousness (Figure 2C). In the extreme case, when one group has an infectiousness value of 1 and a susceptibility value of 0 (completely resistant hosts), and the other group has a susceptibility of 1 and infectiousness of 0 (completely dead-end hosts), such that they lie at extremes of the negative diagonal in σ, ι trait space, no individuals can both be infected and transmit onwards, resulting in an R_0 value of 0 (Figure 2C).

It should be noted that the bifurcating distribution of points observed at high heterogeneity in Figure 2A is due to the boundaries of σ, ι trait space necessarily restricting the number of viable trait combinations (i.e., where both susceptibility and infectiousness values lie between 0 and 1 for all groups) at higher levels of heterogeneity. In the extreme, there are only two configurations of the two groups in σ, ι trait space that leads to maximal heterogeneity (those lying at opposite extremes of the diagonals in σ, ι trait space), resulting in just two points at the maximal heterogeneity value presented in Figure 2A.

In summary, increasing heterogeneity in the RD model can lead to increasingly divergent R_0 values compared to the homogeneous simulation, where the direction of this divergence (positive or negative) is determined by the population-level covariance between susceptibility and infectiousness. When that covariance equals zero (heterogeneity in either susceptibility or infectiousness, but not both) then R_0 is unchanged even as heterogeneity increases).

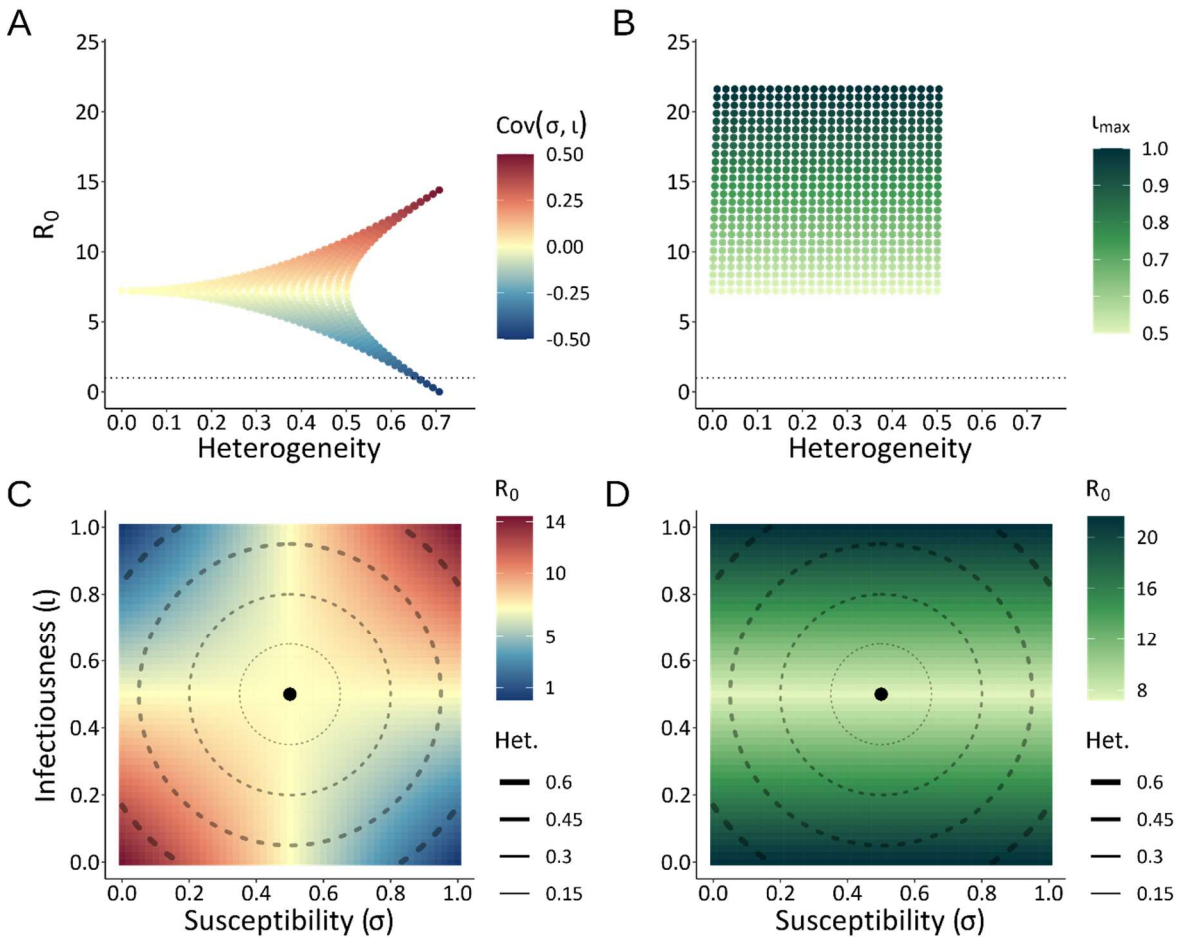

Figure 2. The effect of heterogeneity on R_0. A) RD model. The colour bar shows the covariance between susceptibility (σ) and infectiousness (ι). B) DD model. The colour bar shows the maximum infectiousness ($\iota_{\max}$) value in each simulation. For both (A) and (B) the dotted line shows where R_0 = 1. C) R_0 values for the RD model plotted in σ, ι trait space. D) R_0 values for the DD model plotted in σ, ι trait space. For both (C) and (D) the centre point is the centroid at $\sigma = \iota = 0.5$, the colour bars show R_0 values, the concentric dashed circles show different levels of heterogeneity, and the positions of the subpopulations are mirrored across the centroid ($\sigma_2 = 1 - \sigma_1$ and $\iota_2 = 1 - \iota_1$). Note that the R_0 scales differ in (C) and (D).

Donor-dependent

The DD model produces distinctly different results from the RD model. The overall pattern shows that increasing heterogeneity cannot reduce R_0 relative to the homogenous case (Figure 2B), although R_0 may remain unchanged with increasing heterogeneity. In particular, changes in susceptibility alone do not affect R_0, whereas changes in infectiousness do.

The driver of R_0 for the DD model is the maximum infectiousness value in the population (Figure 2D, Supplementary Equation (S13)), and R_0 is independent of susceptibility because, assuming equal susceptible group sizes, it has a fixed mean value across the population (details in SI). Figure 2D shows that R_0 changes only along the infectiousness axis, and susceptibility trait values do not affect R_0. This means that heterogeneity can be increased by changing susceptibility trait values, but in the absence of changes in infectiousness, R_0 will stay equal to that of the homogenous case. Equally, for the same overall degree of heterogeneity (i.e., vertical slice in Figure 2B) an increase in heterogeneity in infectiousness (and therefore a necessary decrease in heterogeneity in susceptibility to retain the same overall heterogeneity value) will increase R_0. It should be noted that susceptibility can play a role in determining R_0 under a DD scenario, but only when the initial susceptible group abundances are not equal (see SI).

In summary, these results show that in the DD scenario, increasing heterogeneity leads to the potential for increasing R_0 values compared to the homogeneous case, driven by the maximum infectiousness value in the population.

Overall, while both the RD and DD models demonstrate that increasing heterogeneity can lead to increasingly divergent R_0 values compared to the homogeneous case, the driver of those R_0 values differs between the two models. Under the RD scenario, R_0 is driven by covariation between susceptibility and infectiousness, while under the DD scenario R_0 is driven by the maximum infectiousness in the population.

Equilibrium analysis: Change in heterogeneity

To understand how epidemic progress affects population-level heterogeneity, initial heterogeneity and its value at equilibrium were compared. For both the RD and DD models there is generally very little change in population-level heterogeneity throughout the epidemic (Figure 3).

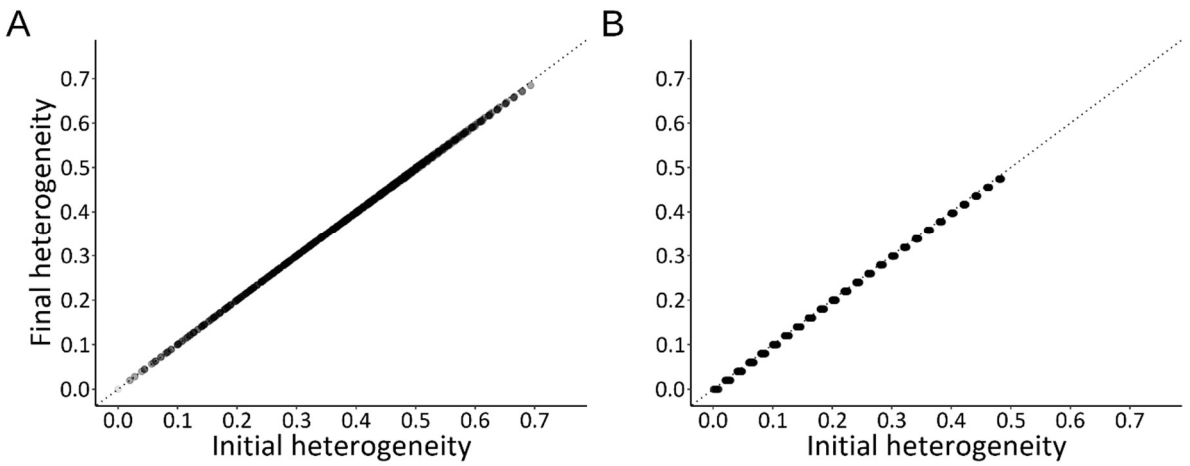

Figure 3. Change in heterogeneity from the initial group values to their equilibrium values (the dotted line shows $y = x$ in both panels). A) RD model, B) DD model. Each point represents one simulation; points are shaded such that darker points represent multiple overlapping points.

Equilibrium analysis: Total host abundance

Equilibrium host abundance generally increases with increasing initial heterogeneity, as does the variability in equilibrium abundance, in both the RD (Figure 4A) and DD (Figure 4B) models. However, the specific relationships between host abundance and heterogeneity differ between the two scenarios.

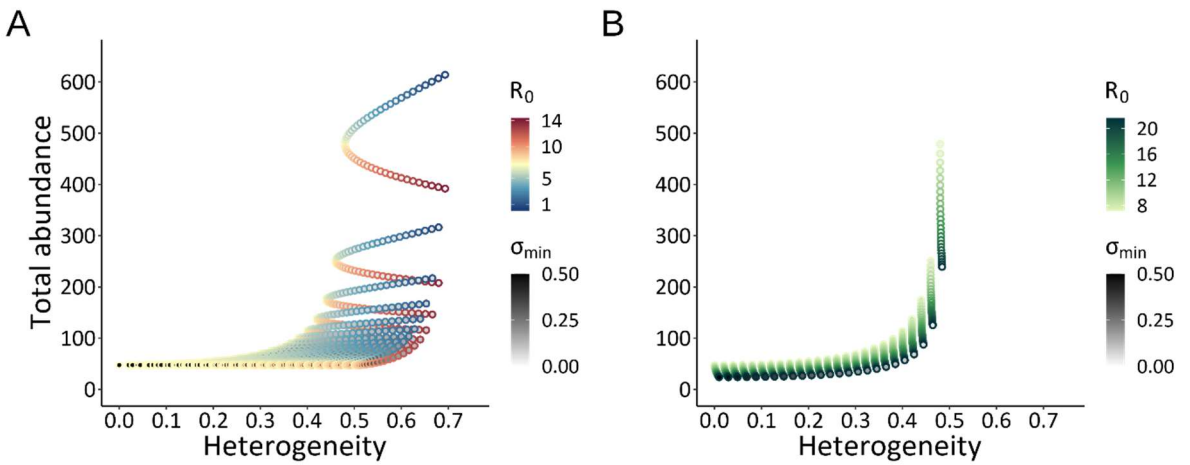

Figure 4. Effect of initial heterogeneity on total host abundance at equilibrium. A) RD model. B) DD model. In both panels the colour bar shows the R_0 value for each simulation, corresponding to the

outline of each point, and the greyscale bar shows the minimum population-level susceptibility value corresponding to the fill of each point.

Recipient-dependent

Under RD infectiousness, heterogeneity affects host equilibrium abundance in a complex manner (Figure 4A). Equilibrium abundances are grouped into parabolic 'clusters' where each cluster has increasing and decreasing equilibrium abundances that diverge from a baseline abundance as heterogeneity increases. These clusters are determined by the minimum susceptibility value in the simulation; each simulation in a cluster has the same population-level minimum susceptibility value (and therefore also the same maximum susceptibility value). The clusters are ordered based on those minimum susceptibility values, with the clusters having the highest abundances comprising simulations with the lowest minimum susceptibility values; populations with low minimum susceptibility values result in fewer individuals moving into infected compartments where they are exposed to parasite-induced mortality (α), thus increasing overall abundance.

The within-cluster divergence seen with increasing heterogeneity for the RD model is due to increasingly divergent infectiousness values in the population. In σ, ι trait space, all the simulations within a cluster have the same pair of σ values for the two groups in the population, so an increase in heterogeneity is achieved by divergence in the two infectiousness values. This divergence in infectiousness values, and thus increase in heterogeneity, leads to changes in R_0 within a cluster and subsequently impacts equilibrium host abundance; high R_0 values lead to lower abundances (the lower red tail of a cluster), while low R_0 values lead to higher abundances (the upper blue tail of a cluster).

Donor-dependent

Although there are once again clusters determined by the minimum susceptibility value within a simulation, these clusters are near-vertical lines, suggesting that heterogeneity does not play much of a role (Figure 4B). Like the RD model, within-cluster host equilibrium abundances are maximised when R_0 is minimised, which occurs at the lowest maximum population-level infectiousness value. Increasing maximum infectiousness for a given cluster increases R_0, and so reduces equilibrium host abundance.

Finally, the DD model generally shows a lower maximum equilibrium host abundance than the RD model because the maximum R_0 values for the DD model are higher than the RD model.

Discussion

Our results show that the infectiousness determination scenario, which determines how infectious hosts become post-infection, alters the relationships between host heterogeneity in susceptibility and infectiousness and various epidemiological outcomes, potentially driving opposing effects of increasing heterogeneity. While existing theory shows that host heterogeneity in susceptibility and infectiousness can affect population-level parasite transmission (e.g. [18]), our findings clarify that these effects differ considerably depending on whether Recipient-dependent (RD) or Donor-dependent (DD) scenarios are assumed.

We showed that while R_0 changes with increasing heterogeneity in both models, both the drivers and direction of those changes differ considerably between the two models. The RD model shows divergent R_0 values as heterogeneity increases, either increasing or decreasing from the homogenous case, determined by the covariance between susceptibility and infectiousness. This finding is supported by previous modelling; three models of vector-borne disease transmission which incorporated host heterogeneity in susceptibility and infectiousness, and which assumed that infectiousness was an inherent trait of the host (*i.e.* RD), found that positive covariance between heterogeneities led to an increase in R_0 relative to the homogeneous case, while negative covariance led to a decrease in R_0 [14, 39, 40]. Thus, with RD determination of infectiousness, population-level covariance between host susceptibility and infectiousness determines R_0.

In contrast, the DD model results in R_0 values that are determined by the maximum infectiousness in a population, such that R_0 increases as heterogeneity in infectiousness increases; heterogeneity in susceptibility is largely irrelevant for the DD model, only becoming relevant if abundances differ considerably between groups. Though there are fewer studies which consider scenarios like the DD model presented here, one example is the hypothesis that the propagation pattern of COVID-19 might be explained by superspreaders tending to generate new superspreaders, for example through a dose-dependent effect [20]. A previous model exploring how R_0 responded to this scenario, relative to a null model in which superspreaders appeared randomly in a population, showed that R_0 increases as the probability that a superspreader generates additional superspreaders increases [19]. Thus, moving from a null model to one similar to DD increased R_0, suggesting that DD infectiousness tends to increase R_0, which aligns with the finding presented here.

Interestingly, despite what we were expecting, we did not find a noticeable divergence between the two models in how population-level heterogeneity changed during the epidemiological process. We expected to see a loss of heterogeneity in the DD model over time because the infected subpopulation with the highest infectiousness value in the population becomes dominant as the epidemic

384 progresses, ultimately excluding less infectious donors. However, heterogeneity is calculated by taking
385 the mean, abundance-weighted distance, of the subpopulations to the centroid. Thus, despite the DD
386 model losing infected subpopulations at equilibrium (and leading to maximally infectious hosts over
387 time), the weighting of the heterogeneity score with the generally larger susceptible subpopulations
388 ensures that there is no considerable loss in heterogeneity at equilibrium.

389 In contrast, the consequences of heterogeneity for equilibrium total host abundances are
390 unexpectedly different between the two scenarios. Though in both the RD and DD models host
391 abundance tends to increase with increasing heterogeneity, heterogeneity has less influence on the
392 equilibrium host abundance in the DD model when compared to the RD model. Furthermore, for a
393 given susceptibility value (i.e., within a cluster) the infectiousness scenario determines whether there
394 are divergent (RD) or monotonic (DD) changes in equilibrium host abundance, a pattern that becomes
395 more notable at higher levels of heterogeneity.

396 Empirical examples of the RD and DD scenarios can be found in the literature. Matching assumptions
397 of the RD model, the nutritional status of canaries can affect their subsequent infectiousness with
398 avian malaria [41]. And in a slightly more complex example, rabbits infected with myxoma virus were
399 shown to be more susceptible to nematode infection and therefore more infectious with respect to
400 the nematode than were rabbits without myxoma virus [42]. Thus, a trait of the rabbit (*i.e.* myxoma
401 infection status) determined its infectiousness with respect to the nematode. As an example matching
402 the DD scenario, calves infected with three different viral doses of bovine viral diarrhoea virus (BVDV)
403 were most infectious when given the highest viral dose, due to a longer infectious period [43], and
404 similar patterns have been found with a number of other animals [44-46].

405 In reality, host-parasite systems are unlikely to be fully described by either the RD or DD models,
406 instead likely falling somewhere between the two. For instance, though the calves challenged with
407 the highest dose of BVDV had a higher infectiousness than other treatments, there was still within-
408 group heterogeneity in infectiousness [43]. This within-group heterogeneity may have been caused
409 by traits inherent to the individual calves, suggesting that while this host-parasite system might be
410 best described by DD infectiousness there are still aspects of RD infectiousness at play. The reverse
411 can also be true. For example, although rabbits may be more infectious with respect to nematodes
412 when also infected with myxoma [42], aligning with RD infectiousness, there may still be some DD
413 infectiousness involved. Specifically, the nematode spreads to other hosts when its eggs are released
414 into the environment in a rabbit's faeces, hatch into larvae and are then eaten by another rabbit [42].
415 So, the chance of a rabbit becoming more infectious is higher when it becomes infected by a rabbit
416 with a high infectiousness, because a highly infectious rabbit will leave many nematode eggs to hatch

417 in a patch of the environment, with the majority likely to infect the same host at the same time. Thus,
418 this susceptible rabbit will then become highly infectious in turn. As such it is likely that the RD and
419 DD scenarios represent two ends of a spectrum, where most real-world host-parasite systems will
420 exist somewhere in between them. This would suggest that in most cases R_0 will be affected by both
421 the covariance between susceptibility and infectiousness as well as the maximum infectiousness in
422 the population, though which of these two measures is more influential will depend on where on the
423 spectrum of IDSs that specific host-parasite system exists.

424 Overall, the models we have presented are an important step in progressing the theory of epidemics
425 in heterogeneous populations. In particualr they demonstrate how the infectiousness determining
426 scenario can change epidemiological outcomes considerably and must therefore be explicitly
427 considered when modelling host heterogeneities in the parasite transmission process.

Acknowledgements

JAC was funded via a PhD studentship from the 'Adapting to the Challenges of a Changing Environment (ACCE)' Doctoral Training Partnership funded by the Natural Environment Research Council (NERC) (Grant NE/S00713X/1).

References

[1] VanderWaal, K.L. & Ezenwa, V.O. 2016 Heterogeneity in pathogen transmission: mechanisms and methodology. *Functional Ecology* **30**, 1606-1622. (doi: 10.1111/1365-2435.12645).

[2] Woolhouse, M.E., Dye, C., Etard, J.-F., Smith, T., Charlwood, J., Garnett, G., Hagan, P., Hii, J., Ndhlovu, P. & Quinnell, R. 1997 Heterogeneities in the transmission of infectious agents: implications for the design of control programs. *Proceedings of the National Academy of Sciences* **94**, 338-342. (doi: 10.1073/pnas.94.1.338).

[3] Lloyd-Smith, J.O., Schreiber, S.J., Kopp, P.E. & Getz, W.M. 2005 Superspreading and the effect of individual variation on disease emergence. *Nature* **438**, 355-359. (doi: 10.1038/nature04153).

[4] Lemieux, J.E., Siddle, K.J., Shaw, B.M., Loreth, C., Schaffner, S.F., Gladden-Young, A., Adams, G., Fink, T., Tomkins-Tinch, C.H. & Krasilnikova, L.A. 2021 Phylogenetic analysis of SARS-CoV-2 in Boston highlights the impact of superspreading events. *Science* **371**, eabe3261. (doi: 10.1126/science.abe3261).

[5] McCallum, H., Fenton, A., Hudson, P.J., Lee, B., Levick, B., Norman, R., Perkins, S.E., Viney, M., Wilson, A.J. & Lello, J. 2017 Breaking beta: deconstructing the parasite transmission function. *Philosophical Transactions of the Royal Society B: Biological Sciences* **372**, 20160084. (doi: 10.1098/rstb.2016.0084).

[6] Dwyer, G., Elkinton, J.S. & Buonaccorsi, J.P. 1997 Host heterogeneity in susceptibility and disease dynamics: tests of a mathematical model. *The American Naturalist* **150**, 685-707. (doi: 10.1086/286089).

[7] Matthews, L., McKendrick, I.J., Ternent, H., Gunn, G., Synge, B. & Woolhouse, M. 2006 Super-shedding cattle and the transmission dynamics of *Escherichia coli* O157. *Epidemiology & Infection* **134**, 131-142. (doi: 10.1017/S0950268805004590).

[8] Streicker, D.G., Fenton, A. & Pedersen, A.B. 2013 Differential sources of host species heterogeneity influence the transmission and control of multihost parasites. *Ecology Letters* **16**, 975-984. (doi: 10.1111/ele.12122).

[9] Stephenson, J.F., Young, K.A., Fox, J., Jokela, J., Cable, J. & Perkins, S.E. 2017 Host heterogeneity affects both parasite transmission to and fitness on subsequent hosts. *Philosophical Transactions of the Royal Society B: Biological Sciences* **372**, 20160093. (doi: 10.1098/rstb.2016.0093).

[10] Barlow, N.D. 2000 Non-linear transmission and simple models for bovine tuberculosis. *Journal of Animal Ecology* **69**, 703-713. (doi: 10.1046/j.1365-2656.2000.00428.x).

[11] Coutinho, F.A.B., Massad, E., Lopez, L.F., Burattini, M.N., Struchiner, C.J. & Azevedo-Neto, R.S.d. 1999 Modelling heterogeneities in individual frailties in epidemic models. *Mathematical and Computer Modelling* **30**, 97-115. (doi: 10.1016/S0895-7177(99)00119-3).

[12] White, L.A., Forester, J.D. & Craft, M.E. 2018 Covariation between the physiological and behavioral components of pathogen transmission: host heterogeneity determines epidemic outcomes. *Oikos* **127**, 538-552. (doi: 10.1111/oik.04527).

[13] Kong, L., Wang, J., Han, W. & Cao, Z. 2016 Modeling heterogeneity in direct infectious disease transmission in a compartmental model. *International Journal of Environmental Research and Public Health* **13**, 253. (doi: 10.3390/ijerph13030253).

[14] Vazquez-Prokopec, G.M., Perkins, T.A., Waller, L.A., Lloyd, A.L., Reiner Jr, R.C., Scott, T.W. & Kitron, U. 2016 Coupled heterogeneities and their impact on parasite transmission and control. *Trends in Parasitology* **32**, 356-367. (doi: 10.1016/j.pt.2016.01.001).

[15] Hickson, R. & Roberts, M. 2014 How population heterogeneity in susceptibility and infectivity influences epidemic dynamics. *Journal of Theoretical Biology* **350**, 70-80. (doi: 10.1016/j.jtbi.2014.01.014).

[16] Yates, A., Antia, R. & Regoes, R.R. 2006 How do pathogen evolution and host heterogeneity interact in disease emergence? *Proceedings of the Royal Society B: Biological Sciences* **273**, 3075-3083. (doi: 10.1098/rspb.2006.3681).

[17] Miller, J.C. 2007 Epidemic size and probability in populations with heterogeneous infectivity and susceptibility. *Physical Review E* **76**, 010101. (doi: 10.1103/PhysRevE.76.010101).

[18] Lloyd, A.L., Kitron, U., Perkins, T.A., Vazquez-Prokopec, G.M. & Waller, L.A. 2020 The basic reproductive number for disease systems with multiple coupled heterogeneities. *Mathematical Biosciences* **321**, 108294. (doi: 10.1016/j.mbs.2019.108294).

[19] Wanelik, K.M., Begon, M., Fenton, A., Norman, R.A. & Beldomenico, P.M. 2023 Positive feedback loops exacerbate the influence of superspreaders in disease transmission. *iScience* **26**. (doi: 10.1016/j.isci.2023.106618).

[20] Beldomenico, P.M. 2020 Do superspreaders generate new superspreaders? A hypothesis to explain the propagation pattern of COVID-19. *International Journal of Infectious Diseases* **96**, 461-463. (doi: 10.1016/j.ijid.2020.05.025).

[21] Stewart Merrill, T.E., Rapti, Z. & Cáceres, C.E. 2021 Host controls of within-host disease dynamics: insight from an invertebrate system. *The American Naturalist* **198**, 317-332. (doi: 10.1086/715355).

[22] Anderson, R.M. & May, R.M. 1991 *Infectious Diseases of Humans*, Oxford University Press.

[23] Begon, M., Bennett, M., Bowers, R.G., French, N.P., Hazel, S. & Turner, J. 2002 A clarification of transmission terms in host-microparasite models: numbers, densities and areas. *Epidemiology & Infection* **129**, 147-153. (doi: 10.1017/S0950268802007148).

[24] Ben-Ami, F., Regoes, R.R. & Ebert, D. 2008 A quantitative test of the relationship between parasite dose and infection probability across different host–parasite combinations. *Proceedings of the Royal Society B: Biological Sciences* **275**, 853-859. (doi: 10.1098/rspb.2007.1544).

[25] Laliberté, E. & Legendre, P. 2010 A distance-based framework for measuring functional diversity from multiple traits. *Ecology* **91**, 299-305. (doi: 10.1890/08-2244.1).

[26] Olusoji, O.D., Barabás, G., Spaak, J.W., Fontana, S., Neyens, T., De Laender, F. & Aerts, M. 2023 Measuring individual-level trait diversity: a critical assessment of methods. *Oikos* **2023**, e09178. (doi: 10.1111/oik.09178).

[27] Heffernan, J.M., Smith, R.J. & Wahl, L.M. 2005 Perspectives on the basic reproductive ratio. *Journal of the Royal Society Interface* **2**, 281-293. (doi: 10.1098/rsif.2005.0042).

[28] Roberts, M. 2007 The pluses and minuses of R0. *Journal of the Royal Society Interface* **4**, 949-961. (doi: 10.1098/rsif.2007.1031).

[29] Diekmann, O., Heesterbeek, J. & Roberts, M.G. 2010 The construction of next-generation matrices for compartmental epidemic models. *Journal of the Royal Society Interface* **7**, 873-885. (doi: 10.1098/rsif.2009.0386).

[30] R Core Team. 2022 R: A language and environment for statistical computing. (Vienna, Austria, R Foundation for Statistical Computing.

[31] Wickham, H. 2016 ggplot2: Elegant Graphics for Data Analysis. (Springer-Verlag New York.

[32] Pedersen, T.L. 2022 ggforce: Accelerating 'ggplot2'. (R package version 0.4.1 ed.

[33] Wickham, H. & Seidel, D. 2022 scales: Scale Functions for Visualization. (R package version 1.2.1 ed.

[34] Qiu, Y. 2022 showtext: Using Fonts More Easily in R Graphs. (R package version 0.9-5 ed.

[35] Schulz, A. 2021 pBrackets: Plot Brackets. (R package version 1.0.1 ed.

[36] Pedersen, T.L. 2022 patchwork: The Composer of Plots. (R package version 1.1.2 ed.

[37] Meschiari, S. 2022 latex2exp: Use LaTex Expression in Plots. (R package version 0.9.6 ed.

[38] Wolfram Research Inc. 2022 Mathematica. (Champaign, Illinois, Wolfram Research Inc.

[39] Koella, J.C. 1991 On the use of mathematical models of malaria transmission. *Acta Tropica* **49**, 1-25. (doi: 10.1016/0001-706X(91)90026-G).

[40] Dietz, K. 1980 Models for vector-borne parasitic diseases. In *Vito Volterra Symposium on Mathematical Models in Biology* (pp. 264-277, Springer.

[41] Cornet, S., Bichet, C., Larcombe, S., Faivre, B. & Sorci, G. 2014 Impact of host nutritional status on infection dynamics and parasite virulence in a bird-malaria system. *Journal of Animal Ecology* **83**, 256-265. (doi: 10.1111/1365-2656.12113).

532 [42] Cattadori, I.M., Albert, R. & Boag, B. 2007 Variation in host susceptibility and infectiousness
533 generated by co-infection: the myxoma–*Trichostrongylus retortaeformis* case in wild rabbits. *Journal*
534 *of the Royal Society Interface* **4**, 831-840. (doi: 10.1098/rsif.2007.1075).
535 [43] Strong, R., La Rocca, S.A., Paton, D., Bensaude, E., Sandvik, T., Davis, L., Turner, J., Drew, T.,
536 Raue, R. & Vangeel, I. 2015 Viral dose and immunosuppression modulate the progression of acute
537 BVDV-1 infection in calves: evidence of long term persistence after intra-nasal infection. *PloS One* **10**,
538 e0124689. (doi: 10.1371/journal.pone.0124689).
539 [44] Zarkov, I. 2012 The importance of inoculation dose of avian H6N2 influenza a virus on virus
540 shedding of *Anas plathyrynchos* ducks after induced generalised infection. *Trakia Journal of Sciences*
541 **10**, 58-61.
542 [45] Mumford, J.A., Hannant, D. & Jessett, D. 1990 Experimental infection of ponies with equine
543 influenza (H3N8) viruses by intranasal inoculation or exposure to aerosols. *Equine Veterinary Journal*
544 **22**, 93-98. (doi: 10.1111/j.2042-3306.1990.tb04217.x).
545 [46] Gaskell, R. & Povey, R. 1979 The dose response of cats to experimental infection with feline viral
546 rhinotracheitis virus. *Journal of Comparative Pathology* **89**, 179-191. (doi: 10.1016/0021-
547 9975(79)90057-4).

548